Morphological stabilization, destabilization, and open-end closure during carbon nanotube growth mediated by surface diffusion

Oleg A. Louchev,* Yoichiro Sato, and Hisao Kanda
Advanced Materials Laboratory, National Institute for Materials Science, 1-1 Namiki, Tsukuba, Ibaraki 305-0044, Japan
(Received 26 April 2001; revised manuscript received 22 April 2002; published 18 July 2002)

In this paper, the growth stability of open-ended carbon nanotubes mediated by surface diffusion on the lateral surface of the nanotube is considered in detail. Nanotube growth and destabilization is viewed as a competition of two processes at the open growth edge: (i) hexagon formation sustaining the continuous growth of the regular hexagonal network, and (ii) thermally activated pentagon formation, which causes inward bending of the nanotube wall resulting in end closure, i.e., growth termination. The edge of the open-ended nanotube, if it is fed by a sufficiently large surface diffusion flux, may remain stable even without extrinsic stabilizing effects. The closure of the open end of the growing nanotube is shown to happen whenever a change in the growth conditions (temperature, carbon vapor pressure, or surface area from which the open end is fed) decreases the surface diffusion flux, and the characteristic time for new atom arrival on the edge becomes larger than the characteristic time for pentagon defect formation. These kinetic effects are also shown to define the transition from single wall to multiwall nanotube growth. Additionally, the effect of surface diffusion feeding nanotube growth from behind the growth interface is shown to stabilize open edge morphology, effectively smoothing the growth perturbations which may be caused by diffusion-limited aggregation at the edge.

DOI: 10.1103/PhysRevE.66.011601 PACS number(s): 81.10.Aj, 81.07.De

I. INTRODUCTION

Since the discovery of nanotubes (NT) and first results on their synthesis and structural characterization, the mechanism of growth kinetics of these structures has remained at the nexus of experimental and theoretical studies [1–50]. The open-end growth model, founded on experimental observations [2,5,6–8], assumes that NTs grow by addition of atoms into the hexagonal network at the edges of the open end and seems to be the most probable mechanism of NT growth. A second model assumes that NT growth proceeds via the addition of atoms into the closed cap followed by incorporation into the hexagonal network [9,10]. However, this model appears implausible given a molecular dynamics study [11] which has shown that the impinging atoms do not incorporate into the hexagonal network, instead forming a disordered structure at the tip. A subsequent model for catalytically grown NTs [23] assumes that C atoms precipitate from a metal nanoparticle supersaturated with carbon, evolving into the formation of a hexagonal structure at the root. This mechanism involves an additional growth limiting step: diffusion of C through the metal particle, which, due to the low diffusion coefficients in bulk matter should give significantly lower growth rates compared with the surface diffusion growth model [18], and, as our recent study [21] shows, has a further restriction associated with the supersaturation of the nanoparticle surface with C.

In the open-end growth model it was originally assumed that the atoms incoming from gas or plasma are captured at the edges by dangling covalent bonds [2], thereby explaining the growth anisotropy of NTs. It has also been proposed that this anisotropy may be caused by differences in impinging fluxes in arc discharge synthesis [13]. In contrast, we believe that NT growth is mediated by an additional process of surface diffusion, which directs atoms that have adsorbed onto the NT surface and onto the underlying substrates at which the NT may be rooted [14–18,21] to the growth edge. Within the surface diffusion model, growth anisotropy appears as an intrinsic effect of NT formation valid for all techniques [18]. Consideration of NT growth within the continuum surface diffusion model [14] has also provided simple explanations for various effects observed in NT studies [15–18,21]. For instance, the effect of surface diffusion, directing to the growth edges adatoms from large surface areas, explains why NTs are not filled through the opening during growth [14,18]. An estimate based upon a microenergetics study [19] shows that for the case of C nanotubes the surface diffusion length may attain the scale of 1 μm for experimental growth temperatures. The surface diffusion model shows also that formation of enclosed shell structures called ''bamboo structures'' may be caused by inequality of surface diffusion fluxes feeding the growth of different layers [15,17,18]. This model provides an explanation for the formation of NT sandwich structures with separated C and BN phases [16]. This model also provides insight into the formation of multiwall nanotubes (MWNT) and transition to the surface amorphization mode [17]. It has also been suggested that surface diffusion is the mechanism which is responsible for NT growth by the ball milling technique [20] and carbon nanotube forest growth by chemical vapor deposition techniques [21].

This paper addresses one of the most debated questions of NT growth kinetics–open-end stabilization/destabilization and closure. We refocus here on this issue by considering the growth of an open-ended NT within the framework of the surface diffusion model. The paper is structured as follows. Section II is devoted to the general discussion of the con-

*Corresponding author.
Electronic mail: louchev.oleg@nims.go.jp

tinuum surface diffusion approximation and its applicability to NT growth kinetics and the issue of open edge stability, outlining major contradictions between different models. Section III details a mechanism for kinetic competition between pentagon and hexagon formation and various implications of this mechanism for NT end closure, formation of enclosed MWNT shell structures, transition from single-wall nanotube (SWNT) to MWNT formation, and postnucleation edge stabilization. Section IV is devoted to the intrinsic stabilization of the open edge provided by surface diffusion against diffusion-limited aggregation. Section V summarizes the main conclusions of our study.

II. THE PROBLEM OF NANOTUBE GROWTH AND OPEN-END STABILITY

A. The continuum surface diffusion model of nanotube growth

Prior to considering the problem of NT edge stability let us discuss in detail the continuum surface diffusion approximation used in the following analysis. First, let us note that in contrast to the case of diffusion in gases, where random walk behavior and migration statistics are defined by the mean free path, in surface diffusion the random walk step and migration statistics are defined by the separation between the adsorption sites (local surface energy wells) corresponding to the interatomic distance on the underlying substrate, $a_0 \cong 0.1$ nm, and not by the adatom separation $\approx 1/\sqrt{n}$ (n is the surface concentration of adatoms). Moreover, even if the adatom is alone on the surface, its random walk migration over distance l is defined by the characteristic diffusion time

$$\tau_{\mathrm{dif}} \approx l^2/D_s, \tag{1}$$

which depends on the surface diffusion coefficient, given by

$$D_s \cong a_0^2 \nu \exp(-\delta E_D/k_B T), \tag{2}$$

where $a_0 \cong 0.14$ nm is the interatomic distance, $\nu \approx 3\times 10^{13}$ Hz is the frequency of thermal vibrations, and $\delta E_D \approx 0.13$ eV [19] is the activation energy of surface diffusion for carbon on a NT surface.

For NT lengths $L \gg a_0 \cong 0.14$ nm, the estimation of the surface diffusion flux to the growth edge and related growth rate may be based on the continuum surface diffusion approximation:

$$\partial n/\partial t = D_s \nabla^2 n + Q_{\mathrm{c}} - n/\tau_a, \tag{3}$$

where Q_{c} is the impinging flux of C atoms onto the surface, which depends on the particular NT growth conditions, $\tau_a = \nu^{-1} \exp(E_a/k_B T)$ is the adsorption time, and E_a is the adsorption energy.

This equation may be reduced to a quasi-steady-state approximation,

$$D_s \nabla^2 n + Q_{\mathrm{c}} - n/\tau_a = 0 \tag{4}$$

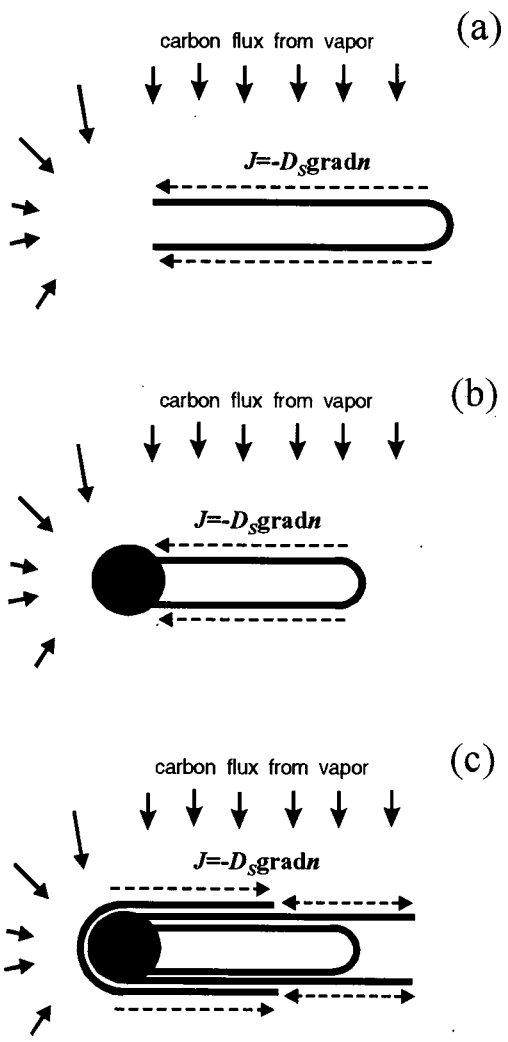

FIG. 1. Schematization of nanotube growth modes: (a) open-ended growth, (b) with liquid catalyst nanoparticle attached at the end when $R_p^2/D_b < 1/(a_0^2 Q_{\mathrm{c}})$, and (c) transition to MWNT formation for $R_p^2/D_b > 1/(a_0^2 Q_{\mathrm{c}})$.

if the characteristic time of stabilization of the concentration field on the NT surface of length L, also defined by Eq. (1), is much lower than (i) the characteristic time of surface geometry change, $L[dL/dt]^{-1}$ (where dL/dt is the NT growth rate), and (ii) the characteristic time of change of C flux impinging onto the NT surface, defined as $Q_{\mathrm{c}}[dQ_{\mathrm{c}}/dt]^{-1}$. That is, Eq. (4) is valid whenever the surface concentration field has enough time to adjust itself to the changing conditions of the system.

The continuum surface diffusion model allows adequate analysis of NT growth even for conditions for which this model at first glance looks inappropriate. Let us consider a one-dimensional (1D) formulation of Eq. (4) for a SWNT starting to grow from a NT nucleus [schematized in Fig. 1(a)–1(c)]. First, we consider the case (a) when the SWNT grows open ended from a semifullerene nucleus. The case of growth with a catalyst nanoparticle, shown in Fig. 1(b), is similar because the contribution of surface diffusion becomes dominant (by comparison with the C flux impinging onto the particle and diffusing through it) as soon as the NT

surface becomes much larger than the nanoparticle surface, i.e., when the NT length becomes much larger than the nanoparticle radius [18]. Moreover, there is an additional physical restriction in feeding NT growth by bulk diffusion through the metal nanoparticle [21] worth briefly mentioning here: the characteristic diffusion time of C through the metal nanoparticle to the NT root given by $\approx {R_p}^2/D_b$ (where D_b is the diffusion coefficient through the particle) should be smaller than the characteristic time of C impingement onto its surface, $\approx 1/(a_0^2 Q_c)$. Numerical estimates of these values, taking into account the fact that melting temperature depends on the surface curvature [21], suggest that the metal nanoparticle should remain in a liquid form during NT growth to allow a fast sink of C atoms by bulk diffusion through the nanoparticle to the NT edge in order to inhibit surface supersaturation with C. This agrees well with the recent thermal analysis of catalyst nanoparticle temperature given by Gorbunov *et al.* [22]. Otherwise, i.e., when $R_p^2/D_b > 1/(a_0^2 Q_c)$, the C content on the nanoparticle surface increases, leading to supersaturation and precipitation directly on the nanoparticle. In this case, the metal nanoparticle serves as a template for the nucleation of a new layer propagating over the first one as schematically shown in Fig. 1(c), leading eventually to MWNT formation around the entrapped metal nanoparticle.

By resolving the 1D surface diffusion problem with $dn/dx=0$ at the NT origin ($x=0$) and the boundary condition at the growth edge, $x=L$,

$$-D_s dn/dx = kn, \tag{5}$$

where $k=a_0/\tau_{\mathrm{inc}}$ is the kinetic constant of incorporation (with the characteristic time τ_{inc} corresponding to the slowest kinetic step at the edge that the adatom overcomes in incorporating into the NT wall), one obtains an ordinary differential equation for NT length,

$$V = dL/dt = -\Omega D_s dn/dx = \frac{\Omega k Q_c \tau_a \sinh(L/\lambda_D)}{\sinh(L/\lambda_D) + (k\lambda_D/D_s)\cosh(L/\lambda_D)}, \tag{6}$$

where Ω is the area per one C atom in the NT wall, and

$$\lambda_D = (D_s \tau_a)^{1/2} = a_0 \exp[(E_a - \delta E_D)/2k_B T] \tag{7}$$

is the surface diffusion length [which may also be defined as $\lambda_D = 2(D_s\tau_a)^{1/2}$].

This equation shows that the continuum surface diffusion approximation works well even for small NT lengths with low surface concentration, reducing asymptotically to the ballistic mode, which is realized when the characteristic time of migration to the edge, Eq. (1), is significantly smaller than the characteristic time of C impingement onto the NT surface, $1/(a_0^2 Q_c)$. That is, expanding Eq. (6) into a Taylor series for $L/\lambda_D \ll 1$, one finds that for the initial stage the growth rate is proportional to NT length,

$$dL/dt \approx \Omega Q_c L, \tag{8}$$

and NT length increases exponentially (or parabolically) with time:

$$L \approx L_0 \exp(\Omega Q_c t) \approx L_0[1 + \Omega Q_c t + 0.5(\Omega Q_c t)^2], \tag{9}$$

where L_0 is the initial NT nucleus length.

For the case when NT length $L \gg \lambda_D$ the growth rate does not depend on L and becomes constant:

$$V \approx \frac{\Omega k Q_c \tau_a}{1 + k\lambda_D/D_s}. \tag{10}$$

Equation (6) allows a simple solution giving an explicit relationship between NT length and growth time:

$$L(t) + \frac{k\lambda_D^2}{2D_s} \ln \frac{\cosh[2L(t)/\lambda_D] - 1}{\cosh[2L_0/\lambda_D] - 1} = L_0 + \Omega \tau_a k \int_0^t Q_c dt, \tag{11}$$

which may be simplified using $\int_0^t Q_c dt = Q_c t$ whenever Q_c may be assumed constant over time.

It should be noted here that the solutions provided by Eq. (11) correspond well with the variety of possible experimental growth modes described in a review paper on growth of hollow graphitic fibers by thermal decomposition of a gas precursor on metal catalyst particles [23] [in treating the growth of a multilayer wall, Eq. (11) should take into account the number of layers in the wall]. In this case a specific dependence of the incorporation constant $k=a_0/\tau_{\mathrm{inc}}$ on the catalyst material should be taken into account. That is, for multiwalled hollow fibers the slowest kinetics step (determining the incorporation rate) most probably corresponds to the transport of C from the edge of the external layer on which the surface diffusion of C species takes place to the core layers through the bulk of the metal particle, giving $\tau_{\mathrm{inc}} \approx d^2/D_b$, where d is the filament wall thickness and D_b is the diffusion coefficient through the particle, which depends on the specific activation energy of the catalyst metal.

This analysis shows that surface diffusion plays a very significant role in feeding NT growth immediately after nucleation, since the flux colliding into the edge is proportional to the edge thickness, whereas surface diffusion flux is proportional to NT length. Even for the cases of kinetically controlled growth $k\lambda_D/D_s \ll 1$, when the growth rate, $V \approx \Omega k Q_c \tau_a$, does not formally depend on the surface diffusion coefficient, it is the surface diffusion which provides a sufficiently large flux of C atoms to the growth edge and therefore does not limit the growth rate. The expansion of Eq. (6) into a Taylor series shows that even under kinetics control, $k\lambda_D/D_s \ll 1$, the initial stage of growth, i.e., when $L/\lambda_D \ll 1$, is described by Eqs. (8) and (9) as long as $L/\lambda_D \ll k\lambda_D/D_s$, and converges to $V \approx \Omega k Q_c \tau_a$ only when the NT length L and related surface diffusion flux, $\propto Q_c L$, become sufficiently large.

The above analysis shows that the continuum surface diffusion model is an effective tool for providing adequate es-

timates of C fluxes to the growth edges even for small NT lengths. This model has the additional advantage of being computationally simple and efficient for low temperatures and for large time ranges, for which molecular dynamics approaches, based even on analytical forms of interatomic potentials, remain so far impractical. This model is potentially able to include and resolve many additional effects. That is, in estimating the impinging C flux we have been using a simplified molecular-kinetics approximation, $Q_c = P/(2\pi m k_B T)^{1/2}$, not specifying whether C atoms or ions are involved, and assuming the flux to be constant during NT growth [15,17]. Analysis of relevant publications related to plasma analysis in arc discharge and laser ablation plumes show that, in reality, the situation is more complicated and several additional effects [13,25–27] may interfere. For instance, in analyzing transport phenomena in arc-discharge synthesis of NTs, Gamally and Ebbesen [13] concluded that there was a non-Maxwellian velocity distribution of C atoms and anisotropy of the related fluxes caused by the presence of the electric field. Thus, by taking into account the surface diffusion influence on NT growth, one may conclude that the E field in the arc-discharge technique is able to accelerate the growth of NTs held perpendicular to it, and also to enhance the nucleation of subsequent layers. The E field may also influence C adatoms surface diffusion transport along the NT, enhancing or inhibiting the growth rate and nucleation of a new layer, depending on the mutual orientation of the E field and the NT. This effect, well known in silicon step-flow growth by molecular beam epitaxy [28], is caused by an effective electric charge of silicon adatoms, and may also be relevant to the case of NT growth. The gas phase transport of NTs during laser ablation synthesis may also influence the process by changing Q_c and also the growth temperature. Moreover, C condensation into NT and other nanostructures will lead to its depletion in the vapor, changing the C flux with time. It is also obvious that the involvement of the electric charge effects of carbon ions and free electrons as well as that of the electric field in the surrounding plasma and on the NT surface may also change the C flux.

The present paper does not address these questions, restricting itself to the stability of open-ended carbon NT growth fed by surface diffusion in terms of surface kinetics of defect formation. To define more clearly the problem that we are going to face here we give in Fig. 2 the solution of Eq. (6) using the simplified molecular-kinetics approximation, $Q_c = P_c/(2\pi m k_B T)^{1/2}$, which is assumed constant during SWNT growth under $T = 1500$ K and $P_c = 10^2$ Pa for the energetics data from Ref. [19]: $E_a \approx 1.8$ eV and $\delta E_D \approx 0.13$ eV. This study does not show that any particular kinetic barrier exists in the transition from the lateral wall onto the edge except that due to surface diffusion, that is,

$$\tau_{\rm inc} \approx \nu^{-1} \exp(\delta E_{\rm inc}/k_B T), \tag{12}$$

where $\delta E_{\rm inc} \approx \delta E_D \approx 0.13$ eV. The related parameters of surface diffusion are $D_s \approx 2.2\times 10^{-7}$ m^2/s and $\lambda_D \approx 0.08\ \mu$m and $k\lambda_D/D_s \approx 6\times 10^2 \gg 1$, corresponding to a diffusion-limited growth mode. Figure 2 shows (a) NT length L, (b) NT growth rate dL/dt, (c) maximal surface concentration of C given by

$$n_{\rm max} = n(0) = Q_c \tau_a \times \left[1 - \frac{(k\lambda_D/D_s)}{\sinh(L/\lambda_D) + (k\lambda_D/D_s)\cosh(L/\lambda_D)}\right], \tag{13}$$

and (d) the ratio of L^2/D_s to L/V, showing the validity of the steady-state approximation.

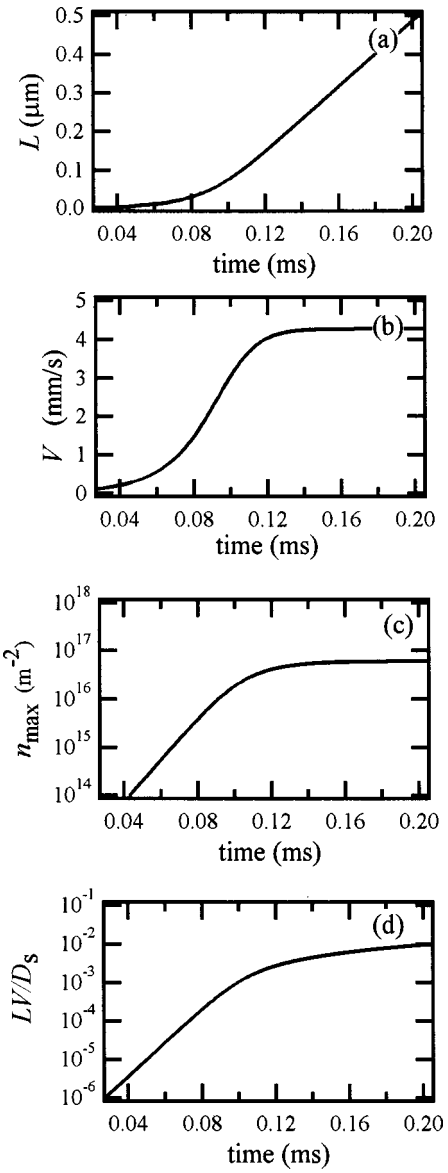

FIG. 2. Analytical solution of SWNT growth parameters as a function of time: (a) SWNT length, (b) growth rate, (c) maximal surface concentration, and (d) criterion of validity of steady-state approximation.

This solution shows that dL/dt [Fig. 2(b)] and $n_{\rm max}$ [Fig. 2(c)] are stabilized after the NT length becomes larger than the surface diffusion length $\lambda_D \approx 0.08\ \mu$m. With time the growth rate becomes constant $V \approx \Omega\ Q_c \lambda_D$ and, in principle,

the SWNT may continue to grow. However, for this particular case the final separation between the adatoms $\approx 1/\sqrt{n_{\max}} \approx 3\,\mathrm{nm} \ll \lambda_D$ meaning that adatoms are able to meet each other prior to desorption and to aggregate, thereby leading to the nucleation of the next layer and to transition to the step-flow growth of MWNTs [17]. However, under lower C vapor pressures the concentration becomes low and the SWNT surface is not prone to secondary nucleation. Thus, from this point of view surface diffusion allows SWNT to grow to a length considerably greater than λ_D. However, this seems to contradict to the experimental data, which indicates that the formation of long SWNTs is feasible only in the presence of metal nanoparticles. This contradiction, combined with the issue of open edge stability/instability with respect to defect formation, causing SWNT closure, is the main focus of our study.

B. The issue of open edge stability

The issue of open-end stability has remained one of the most challenging questions related to the open-ended NT growth, because the open edge appears to be prone to the formation of different types of defects, which alter NT growth. In fact, the conclusion about open-ended NT growth [2] has immediately posed a natural question: how the open-end can remain stable given the dangling covalent bonds present on the growth edges, which should form pentagons and thereby close the end. It was proposed that this stability may be due to a high electric field concentrated at the NT tip, which stabilizes the edge or increases the barrier to its closure [29]. However, it was found that this mechanism would be unable to stabilize an open end at the realistic field strengths [13,30]. Other extrinsic factors, such as growth below the annealing temperature [31], adsorbed hydrogen atoms [32], or catalytic particles [6,33] were proposed to explain this effect. It was suggested that a stabilizing effect on the growth edge can also be caused by the action of catalyst atoms adsorbed on the growth edge providing annealing of pentagon defects [19,34]. Without this annealing the growth of small radius SWNTs of carbon would not be possible because of pentagon formation on the growth edge leading to the tip closure, found both for zigzag and the armchair orientation [35]. It has also been shown that a stabilizing effect, which allows the growth of carbon SWNTs (but only with zigzag orientation), may also be produced by atoms of B [36]. In contrast, the open edge of a carbon SWNT was found by a molecular dynamics study to be quite stable during growth if its diameter exceeds a value of 3 nm even without the action of catalysts [37] (allowing one to understand the lack of narrow SWNTs in noncatalytic growth). However, narrow SWNTs were found to form pentagonal rings on the open edge, closing subsequently in a disordered cap structure [37]. Reference [38] also suggested that a stabilizing effect may also be provided by a repulsive potential of a particle present at the NT end. The stabilization of the NT growth edge has also been suggested to be due to the so-called lip-lip interaction: the presence of carbon atoms bridging the edges of adjacent layers [39]. This effect, providing a significant gain in the surface energy on the growth edge, is suggested to allow a double-walled or multiwalled NT to grow without end closure, whereas SWNTs tend to close up [40,41]. However, in contrast to this, a molecular dynamics study shows that for the case of narrow NTs the lip-lip interaction by itself cannot maintain stability of the open end, which also has a tendency to close up [42]. It should also be noted that in addition to Ref. [37] the possibility of SWNT formation without any metal catalyst is also supported by an experimental observation [43].

Paper [39] suggests that a NT growing from a semifullerene nucleus may evolve into an open-ended SWNT under the action of a catalyst at the edge, or evolve into an open-ended MWNT if in a highly supersaturated C vapor, the new layers form on top of the first layer, and the lip-lip interlayer interaction stabilizing the edge is formed. However, while analyzing the formation of double-walled semifullerene NTs suggested in Ref. [39] we find that the open edge of the first semifullerene layer represents an effective sink for C atoms and dimers impinging into its surface, and due to the surface diffusion of these atoms to the edge followed by their incorporation, the surface concentration is too low to enable the nucleation of the second layer. In effect, the characteristic repetition time at which the C atoms impinge into the surface of a semifullerene NT nucleus, τ_{imp}, depends on the carbon flux Q_{c} as

$$\tau_{\mathrm{imp}} \approx 1/SQ_{\mathrm{c}}, \tag{14}$$

where $S \approx 2\pi R^2$ is the external semifullerene nucleus area subject to the impinging flux of carbon.

Let us compare the above value with the characteristic diffusion time, Eq. (1), using the characteristic length $L \approx \pi R/2$ the adatom has to overcome in reaching the growth edge. That is, for a semifullerenelike NT nucleus with radius $R \approx 0.5$ nm, the characteristic impingement time is $\tau_{\mathrm{imp}} \approx 4\times 10^{-8}$ s at $T=1000$ K for $P_{\mathrm{c}}=100$ Pa (corresponding to graphite source evaporation at $T_{\mathrm{ev}}=3400$ K). In contrast, the typical diffusion time along the path to the edge $L \approx \pi R/2$ gives a value $\tau_{\mathrm{dif}} \approx 4\times 10^{-12}$ s for $D_s \approx 1.4\times 10^{-7}$ m^2/s. Comparing these values one finds that under specified conditions the nucleation of the second layer on the surface of a NT nucleus is quite unlikely because an adatom escapes from the surface to the edge about four orders of magnitude faster than the time taken by the next one to arrive. Even for $P_{\mathrm{c}} \approx 4000$ Pa ($T_{\mathrm{ev}} \approx 4000$ K), $\tau_{\mathrm{imp}} \approx 10^{-9}$ s is still more than two orders of magnitude higher than the diffusion time $\tau_{\mathrm{dif}} \approx 4\times 10^{-12}$ s. However, with increase in length a SWNT may evolve into a MWNT. If a single layer semifullerenelike nucleus of $R=0.5$ nm grows open ended forming a NT of length $L=50$ nm, its surface becomes $S \approx 2\pi RL$, and the characteristic impingement time becomes $\tau_{\mathrm{imp}} \approx 4\times 10^{-10}$ s (for $P_{\mathrm{c}}=100$ Pa), whereas the diffusion time for overcoming the distance $L=50$ nm becomes $\tau_{dif} \approx 2\times 10^{-8}$ s, i.e., larger by more than an order of magnitude. In this case the nucleation of the second layer becomes feasible and successive layer-by-layer nucleation and growth may take place. But even in this case the NT initially grows as a SWNT.

One may argue that in effect the second layer may also nucleate by deposition of large C fragments (present in su-

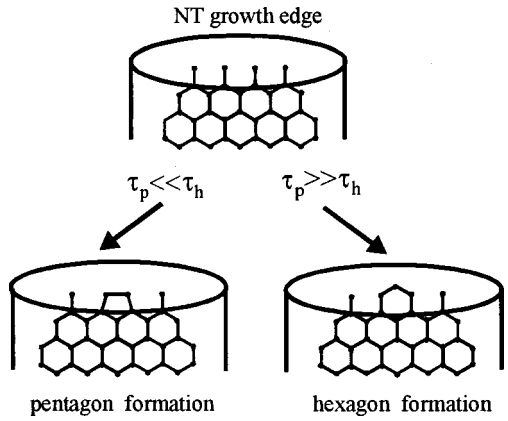

FIG. 3. Schematization of kinetic competition between pentagon and hexagon formation on the open growth edge.

persaturated vapor) which may serve as surface nuclei. The possibility of such an event is undeniable, especially taking into account a recent study, which shows that in a C nanosheet interaction with nanotemplates, a folded configuration around the template surface should be energetically more favorable due to long-range interactions [44]. However, it is obvious that if this happens under all conditions on every NT nucleus, leading to the formation of a new layer on top of the first one, the growth of SWNTs would never be possible. Thus, once again the same question about the open-ended growth model arises: what is the mechanism (a) enabling a SWNT to grow with a stable open edge, at least until the moment when the nucleated second layer catches up with the first one and forms a lip-lip interaction or a catalyst atom/particle adsorbs onto the edge and (b) causing an open-ended nanotube to eventually close up?

III. PENTAGON/HEXAGON COMPETITION AND NANOTUBE FORMATION

A. Kinetic competition between pentagon and hexagon formation

The answer to the problem of open edge stability in NT growth and related issues of end closure, suggested in this paper, follows from a consideration of two basic processes and related characteristic times defined below.

First, NT closure is known to be initiated by the formation of pentagons on the edge [2,5,11,37,38]. The process of pentagon formation, associated with atom reconstruction and change in interatom separations at the edge (Fig. 3) should occur via an activation energy barrier δE_p implying a corresponding time of pentagon formation, τ_p, which depends on growth temperature as

$$\tau_p \approx \nu^{-1} \exp(\delta E_p / k_B T). \tag{15}$$

Every possible path of atom reconstruction on the edge leading to pentagon formation would obviously require a different activation energy δE_p. Let us consider data available for the particular case of armchair NT orientation: Ref. [19] gives the energy levels on the edge corresponding to the C atom position in the hexagon (-7.3 eV) and in the pentagon (-6.3 eV) with the energy barrier from hexagon to pentagon at the level of -4.9 eV. Thus, for the particular case considered in Ref. [19], the activation energy of pentagon formation should have the value of $\delta E_p \approx 7.3-4.9 \approx 2.4$ eV.

Second, the process of pentagon formation on the edge competes with the process of addition to edge sites of new C atoms continuing the formation of a defectless hexagon network. The related time depends on the characteristic interval at which new C atoms are repeatedly fed to the edge sites. The growth of a NT is mainly fed by surface diffusion, which directs to the growth edge atoms impinging into the lateral surface of the NT. Therefore, the time of hexagon formation, depends on the surface diffusion flux, $J_s = -D_s \operatorname{grad} n$, per one edge site,

$$\tau_h \approx \frac{1}{\sqrt{3} a_0 J_s}, \tag{16}$$

which assumes that hexagon formation is limited by the time of a new atom arrival and that the incorporation kinetic time is negligibly small (Ref. [19] shows that the atom approaching the edge does not have any specific activation energy barrier prior to the transition onto the edge).

Thus, if $\tau_p \gg \tau_h$ the formation of the pentagon defects is inhibited by faster hexagon formation, or at least their number is not detrimental to NT formation. In this case the edge stability against pentagon formation may be intrinsically maintained during NT growth without any other extrinsic effect. Otherwise, the NT edge appears to be prone to destabilization by pentagon formation, which initiates end closure.

Let us compare these two times for a semifullerene nucleus with $R = 0.5$ nm. In this case the surface diffusion flux is minimal. For NTs smaller than the surface diffusion length the desorption is negligibly small and the diffusion flux is equal to the ballistic flux into the surface,

$$J_s \approx \frac{S Q_c}{2 \pi R}, \tag{17}$$

where S is the NT surface subject to C flux from vapor. After the nucleation of a semifullerene nucleus, the effective area in which C atoms impinge is $S \approx 3 \pi R^2$, and with an increase in the NT length L it becomes $S \approx 2 \pi R L$ tending finally to the upper possible limit $S \approx 2 \pi R \lambda_D$, where λ_D is the surface diffusion length.

In Fig. 4 these characteristic times are plotted versus the temperature for different values of activation energy of pentagon formation within the range $\delta E_p = 2-2.5$ eV and for $P_c \approx 4000$ Pa ($T_{ev} = 4000$ K). For low T, $\tau_h \ll \tau_p$ and pentagon formation is inhibited by new C atoms diffusing to the edge and forming a regular hexagonal network. In contrast, for higher T, $\tau_h \gg \tau_p$, implying that pentagon defects are formed much faster than hexagons. It is necessary to outline the importance of carbon vapor pressure in maintaining the edge stability. For instance, for $P_c = 4000$ Pa the hexagon formation time is $\tau_h \approx 5 \times 10^{-8}$ s at $T = 1500$ K, which is considerably smaller than the time of pentagon formation,

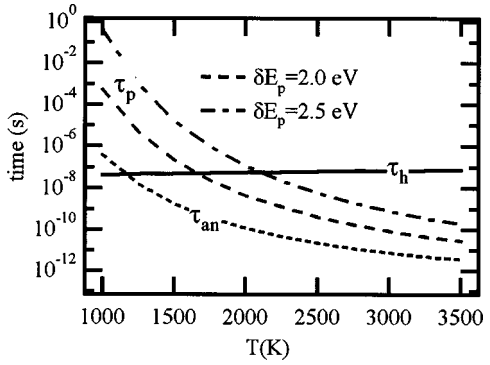

FIG. 4. Dependence of characteristic time of pentagon formation and hexagon formation, which shows that for $P_c \approx 4000$ Pa ($T_{ev} \approx 4000$ K) pentagon formation prevails at high temperatures, whereas hexagon formation prevails at low temperatures.

$\tau_p \approx 2\times10^{-7}$ s ($\delta E_p = 2.0$ eV) and $\tau_p \approx 2\times10^{-5}$ s ($\delta E_p = 2.5$ eV), and edge stability may be maintained. However, for $P_c \approx 4$ Pa ($T_{ev} \approx 3000$ K) $\tau_h \approx 5\times10^{-5}$ s $> \tau_p$ and the edge appears to be prone to pentagon defect formation.

The increase in the NT length and in the lateral surface area S increases the surface diffusion flux to the growth edge, decreasing even further the value of τ_h, and enhancing thereby the stability of the edge against pentagon formation. It is important to emphasize here the significance of surface diffusion, which directs to the growth edge a sufficiently large amount of C atoms even immediately after the nucleation stage. If only the contribution of direct collisions into the edge site from the vapor is taken into account, one finds that the corresponding time $\tau_h \approx 1/a_0^2 Q_c$ is about six times larger than the time corresponding to Eq. (16) for a semifullerene NT nucleus with $R = 0.5$ nm.

One may argue here that pentagon defects may be annealed into regular hexagons; for armchair orientation the corresponding activation energy barrier is shown to be $\Delta E_{an} \approx 6.3-4.9 = 1.4$ eV [19]. The dependence of the corresponding time

$$\tau_{an} \approx \nu^{-1} \exp(\Delta E_{an}/k_B T), \tag{18}$$

given also in Fig. 4, shows that it is significantly smaller than τ_h for high temperatures and has the same order of magnitude near 1200 K. However, regardless of τ_{an}, the annealing of the pentagon also requires the presence of an additional sixth C atom near this defect and, therefore in reality it is also controlled by the rate at which C atoms are fed to the edge by surface diffusion. That is, the real time for the pentagon-hexagon transition, $\tau_{p\to h} \approx \tau_h + \tau_a$, is determined by the highest value, i.e., by Eq. (16) or (18).

This analysis shows that by virtue of the surface diffusion, the edge of the open-ended NT, if it is fed by a sufficiently large surface diffusion flux, may remain stable even without other edge stabilizing effects such as metal catalysts, hydrogen atoms, or lip-lip interaction. Moreover, the dependence of the edge stability on the surface diffusion flux resolves an apparent contradiction between different studies, which show on the one hand that for stabilization of the open end, a catalyst is required for SWNTs [19,39] or lip-lip interaction for MWNTs [40,41], and on the other hand that large diameter SWNT may grow with a stable open end without a catalyst [37], whereas narrow two-layer NTs even with lip-lip interaction close up [42]. Our analysis suggests that the molecular dynamics study [42] of NT growth by direct impingement into the edge performed at 3000 K neglects the effect of surface diffusion whereas suggestions based on microenergetics data [19,39,40] do not take into account the kinetic aspects of the problem. The analysis of typical times involved in the processes of pentagon-hexagon formation allows us to conclude that a NT may grow with open end without other stabilizing effects on the edge whenever it is fed by a sufficiently large surface diffusion flux ($\tau_h \ll \tau_p$), whereas even with the stabilizing effect of lip-lip interaction, a double-wall NT should close up when the surface diffusion flux becomes too small.

B. Nanotube end closure

In general, the closure of a growing open-ended NT may happen whenever the change in the growth conditions (temperature, carbon vapor pressure, and surface area from which the open end is fed) decreases the surface diffusion flux, and the characteristic time of new atom arrival on the edge becomes larger than the characteristic time of pentagon defect formation.

In particular, open-end closure may occur due to a depletion in P_c around the growing NT. Let us assume that at the beginning of growth $P_C \approx 4000$ Pa ($T_{ev} \approx 4000$ K), corresponding to the bulk concentration $n_c = P_c/k_B T \approx 10^{23}$ m^{-3} (at $T = 1500-3000$ K). A SWNT of carbon of $R = 0.5$ nm and $L = 1$ μm contains $N_c \approx 10^{15}$ atoms. This means that the growth of one 1-μm-length NT is able to exhaust the carbon vapor from $N_c/n_c \approx 10$ mm^3 of the surrounding gas volume. The fall in P_c causes a linear decrease in $J_s = -D_s \operatorname{grad} n \propto P_c$, which feeds the growth and, as a consequence, in $\tau_h \propto P_c^{-1}$.

Next, we should indicate another possible route of NT closure. Arc discharge, laser heating, and other techniques of NT synthesis are characterized by high nonuniformity in the concentration and temperature fields in the active synthesis zone, often accompanied by strong convective flows. For instance, during arc-discharge synthesis the temperature nonuniformity may cause natural convection loops, which provide transport of growing NTs through regions with higher and lower temperature and carbon vapor pressure. The changes and oscillations in the temperature and impinging carbon flux may both destabilize open end and initiate its closure. Even the transport of a NT outside the synthesis zone may destabilize the end and close it up. The same arguments allow one to understand why the termination of the synthesis leads to end closure during the final stage of the process. In effect, after the termination of evaporation by arc discharge or laser heating, the thermal energy of the gas and the carbon vapor dissipate. In gases, the dissipation of thermal energy and concentration occurs at the same rate because the thermal diffusivity and the concentration diffusivity have the same order of magnitude. However, in the case

considered the dissipation of carbon vapor takes place simultaneously with vapor condensation into the NTs and other solid structures. Therefore, the carbon vapor concentration in the gas dissipates more rapidly than the thermal energy. Additionally, the released heat of condensation and solid particles having high thermal inertia both decelerate temperature fall. Hence, the rapid fall in P_c will induce a rapid increase in the characteristic time of the hexagon formation compared with that of pentagon formation. This will lead to the situation when at the final stage of the process, pentagon formation will dominate over the formation of new hexagons at the open ends of NTs, causing their closure.

Thus, the formation of long NTs requires continuous evaporation of graphite and effective transfer of carbon vapor into the zone of synthesis, which should be maintained under a considerably lower temperature to inhibit pentagon formation at the edge. This consideration suggests that open-ended NTs tend to close up during the process and especially at the final stage, explaining why, in accordance with the postprocess high-resolution microscopic observations, NTs with closed ends prevail in deposits.

C. Formation of enclosed MWNT shell structures

The destabilization of the growth edge due to decrease in surface diffusion flux also suggests a particular mechanism of MWNT growth into enclosed shells. In the previous publications [15,17] it has been shown that MWNT structures with enclosed shells, frequently observed in NT synthesis, are formed because during layer-by-layer nucleation and growth, every subsequent layer grows faster than the underlying layer and finally catches up with it and, thereby, stops completely the growth of the underlying layer. Based on the estimates made in Sec. II B one finds that the second layer may nucleate when $\tau_{\mathrm{imp}} \ll \tau_{\mathrm{dif}}$. Comparing τ_{dif}, Eq. (1), with τ_{imp}, Eq. (14), one finds that nucleation of the next layer becomes feasible when the length of the first layer $L \gg (D_s/2\pi R Q_c)^{1/2}$. After nucleation the second layer grows initially with about the same rate as the first one [15,17]. However, with increase in L the second layer starts to grow faster, because it is fed, in addition, by surface diffusion from its own surface. Finally, the growth edge of the second layer catches up with the edge of the first layer, leading to the increase in τ_h for the first layer as schematized in Fig. 5(a)–5(d). In effect, before the nucleation of the second layer [Fig. 5(a)] the area feeding the growth by surface diffusion is $S \approx 2\pi R L_1$. The effective area from which the first layer is fed after the nucleation of the first layer is $S = 2\pi R \delta L$, where $\delta L \approx (L_1 - L_2)/2$ is the distance between the first and the second layer [Fig. 5(b)]. When the edge of the second layer gets closer to that of the first one [Fig. 5(c)] the decrease in $S = \pi R(L_1 - L_2)$ results in an increase in τ_h. Hence, the growth of the second layer leads not only to slowing down and complete inhibition of the growth of the underlying layer, it also induces the formation of pentagon defects at the edge of the first layer causing closure [Fig. 5(d)].

In fact, the moment the second layer catches up with the first one, their edges may also undergo lip-lip interaction, and subsequently propagate together [Fig. 5(e)]. The kinetic

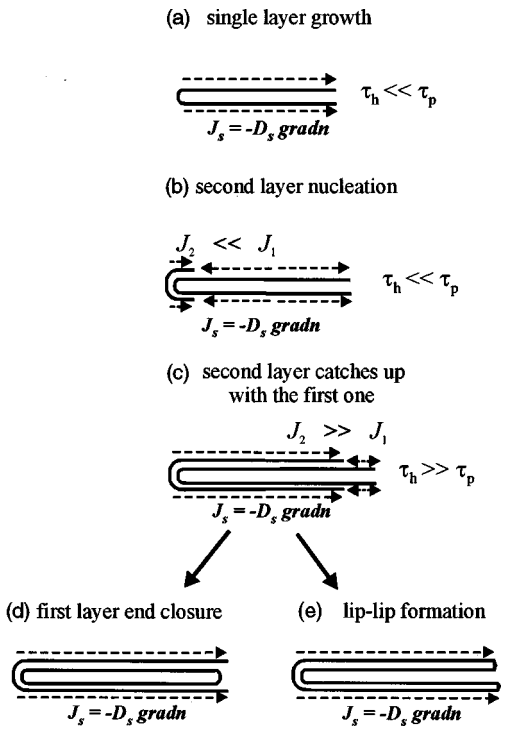

FIG. 5. Schematization of enclosed shell structure formation in MWNT growth: (a) increase in SWNT length; (b) provokes nucleation of the next layer (c), which with time gets closer to the end leading (d) to end closure or (e) to the formation of lip-lip interaction and simultaneous propagation of a two-layer wall.

selection between (i) the closure of the first layer or (ii) interedge lip-lip formation looks to be the result of the competition between two effects. That is, if the edge of the first layer has closed at the moment the second layer finally catches up, the lip-lip formation appears impossible and the second layer propagates, leaving the first one behind. Striking experimental evidence for such behavior is given in Ref. [45]. If the second layer propagates rapidly enough compared with the rate of end closure by pentagon formation, then both layers may form lip-lip bridging and propagate later on simultaneously, under the additional condition that the bridges between the layers provide an effective redistribution of the adatoms coming by surface diffusion to the edge of the external layer onto the edge of the internal layer [17].

In contrast to the above kinetics mode, another scenario of enclosed shell formation, when layer closure initiates nucleation and propagation of the next layer, is also possible. That is, if the growth of the first layer has exhausted the local C vapor, the NT end closes up because of the increase in τ_h. The layer closure cuts off the consumption of carbon on its surface and also in the gas. Thus, after this closure an increase in the carbon vapor concentration should follow, and, as a consequence, the surface concentration n on the lateral surface increases to the level which triggers the nucleation of a new layer, which grows along the surface of the underlying layer until its own closure—which in its turn causes an increase in carbon concentration in vapor, in surface concen-

tration n, nucleation, propagation, and closure of the next layer.

D. Transition from SWNT to MWNT formation

Let us now approach the problem of SWNT formation and the transition to the formation of MWNT. Let us specify the conditions allowing a SWNT to form. Returning to the competition of hexagon and pentagon formation on the edge, the ratio of the characteristic times τ_p/τ_h,

$$\tau_p/\tau_h=\sqrt{3}a_0 J_s \nu^{-1}\exp(\delta E_p/k_B T)>10, \tag{19}$$

represents a reasonable level at which pentagons formed at the edge may not result in NT closure. Hence this condition may be used as a criterion of edge stability against the closure by pentagon formation.

This criterion requires that higher carbon vapor pressure P_c and lower growth temperatures T are necessary to maintain open-end stability. However, this criterion and implied requirements contradict the condition of SWNT formation, which requires (i) lowering P_c and (ii) increasing T in order to maintain low surface concentration on the NT surface and to inhibit surface nucleation of the next layers [17]. Surface nucleation of the second layer may happen if the adatoms are able to overcome the separation distance, which depends on the maximal surface concentration $\lambda_s=1/n_{\max}^{1/2}$. In order to overcome this distance by surface diffusion and to form the nucleus, the adatoms require a time of order of magnitude

$$\tau_{\rm nuc}\approx\frac{N\lambda_s^2}{4D_s}=\frac{N}{4D_s n_{\max}}, \tag{20}$$

where the factor $N\approx\exp(\delta E_{\rm nuc}/k_B T)$ represents the number of surface collisions necessary for adatoms to make a nucleus, overcoming some activation energy barrier $\delta E_{\rm nuc}$. If this time is larger than the time of adsorption, $\tau_a \approx \nu^{-1}\exp(E_a/k_B T)$, the nucleation of the next layer is impossible. Hence, the criterion of the inhibition of secondary nucleation may be formalized as

$$\tau_a/\tau_{\rm nuc}=4D_s n_{\max}\tau_a/N<1. \tag{21}$$

During NT growth the values of surface diffusion flux and of the maximal concentration increase. Resolving the continuous quasi-steady-state approximation for growth mode limited by diffusion, $k\lambda_D/D_s\gg 1$, with $dn/dx=0$ at the NT origin $(x=0)$ and $n=0$ at the edge $(x=L)$, one obtains

$$n_{\max}=n(0)=Q_C\tau_a[1-1/\cosh(L/\lambda_D)] \tag{22}$$

and

$$J_S=-D_S dn/dx_{|x=L}=Q_C\lambda_D\tanh(L/\lambda_D). \tag{23}$$

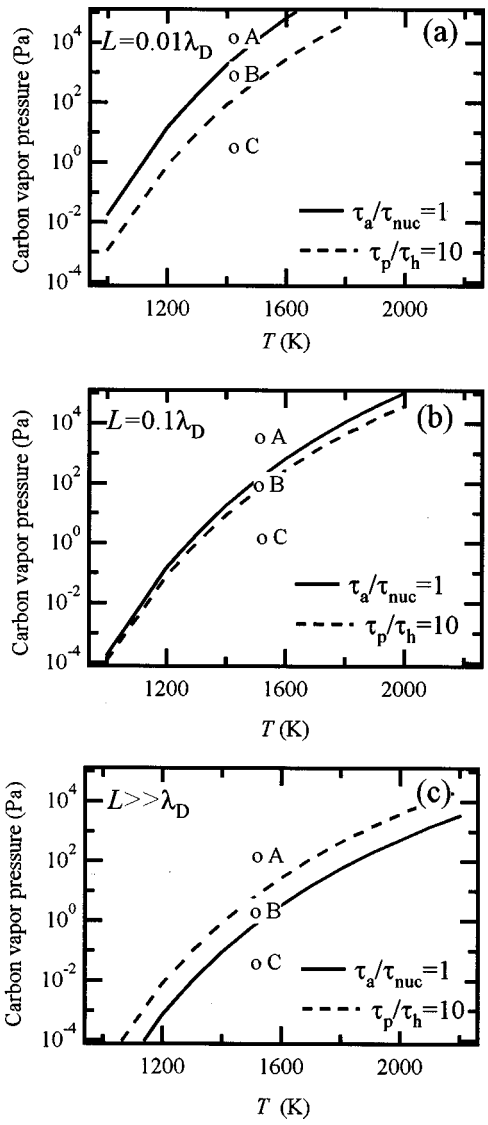

FIG. 6. P_c-T areas corresponding to (i) open-end stability against pentagon defect formation (above broken line) and (ii) the inhibition of secondary nucleation on the surface (below solid line) for different SWNT lengths.

For later discussion let us note that for $L\gg\lambda_D$ one has $J_s\approx Q_c\lambda_D$ and $n_{\max}\approx Q_c\tau_a$, whereas for $L\ll\lambda_D$ one has $J_s \approx Q_c L$ and $n_{\max}\approx 0.5 Q_c\tau_a(L/\lambda_D)^2$.

In Figs. 6(a)–6(c) we show isolines $\tau_p/\tau_h=10$ and $\tau_a/\tau_{\rm nuc}=1$ in coordinates of P_c and T. These isolines define areas of open-end stability against pentagon formation (above the broken lines) and the areas of stability of a SWNT surface against the nucleation of the next layer (below the solid lines). Both criteria depend on the NT length and are given for (a) $L=0.01\lambda_D$, (b) $L=0.1\lambda_D$, and (c) $L\gg\lambda_D$. This figure shows that the smaller the length, the larger the P_c-T area in which the NT may grow with a stable open end and without secondary nucleation (see the cases of $L=0.01\lambda_D$ and $L=0.1\lambda_D$). This is due to the fact that for $L\ll\lambda_D$ the values of τ_p/τ_h are proportional to L and the limiting pressure, corresponding to $\tau_p/\tau_h=10$, is $P_c\propto 1/L$ (shown by the broken line). In contrast, for $L\ll\lambda_D$ the value

of $\tau_a/\tau_{\rm nuc} \propto L^2$ and the limiting pressure, corresponding to $\tau_a/\tau_{\rm nuc}=1$ is $P_c \propto 1/L^2$ (shown by solid line). Therefore, with the increase in SWNT length the P_c-T area corresponding to open-end stability against pentagon formation expands less rapidly compared with the decrease in the P_c-T area corresponding to the stability against secondary nucleation. As a result, as long as SWNTs remain short $L \ll \lambda_D$, there are P_c-T areas in which they can remain stable [points *B* in Figs. 6(a) and 6(b)] against pentagon formation and secondary nucleation. In contrast, for $L \gg \lambda_D$ [Fig. 6(c)] SWNTs become unstable against secondary nucleation (point *A*), pentagon formation on the growth edge (point *C*), or against both of them (point *B*).

Our analysis does not take into account the possible additional effects which may prevent pentagon formation and NT closure. For instance, in the presence of catalyst the edge [19] may maintain stability against pentagon formation even in P_c-T areas below the broken line, enabling SWNTs' growth to lengths considerably larger than that of λ_D. Nevertheless, in the absence of a catalyst or hydrogen atoms in the P_c-T areas below the broken lines, the open end is prone to pentagon formation and should close. After this closure happens the NT may be covered by subsequent layers leading to the formation of MWNTs.

It is important to note here that with increase in SWNT length, the P_c-T area corresponding to stability against pentagon formation and secondary nucleation [shown by point *B* in Figs. 6(a) and 6(b)] shifts to lower C vapor pressures. This corresponds to the general tendency in SWNT synthesis by laser ablation where SWNTs nucleate at high C vapor pressure, but with time they are transported by gas flow to areas of lower C pressure out away from the graphite source. If, finally, these NTs are transported into the P_c-T area corresponding to point C in Fig. 6(c) they may grow into a long SWNT under the action of a metal particle on the edge, or else close themselves up into a shorter NT shell if they grow without a catalyst.

E. Influence of a metal catalyst nanoparticle

This study also provides an explanation as to why the involvement of a metal catalyst nanoparticle would increase the output of NTs and particularly of SWNTs. The presence of metal catalyst atoms or particles at the NT growth edge inhibits the formation of pentagons under pressure-temperature conditions at which, without the catalyst, the NT open edge would be prone to destabilization. The influence of individual metal atoms (Ni) on edge stability has been considered in Ref. [19] based on quantum mechanics calculations. The stabilizing effect of a metal nanoparticle attached to a nanotube end [schematized in Fig. 1(b)] appears to be a simpler explanation. That is, to allow the formation of hexagonal-phase nanotubes, the metal particle should be supersaturated with carbon relative to the hexagonal phase. The equilibrium concentration of any substance in a solvent is $C_{\rm eq} \propto \exp(-\Delta H/k_B T)$, where $\Delta H = E_b - E_s$ is the dissolution heat corresponding to the difference between atom energy in the solid phase, E_b, and that in the solvent, E_s. The value of E_b is larger for regular hexagons as compared with pentagons, whereas E_s for C atoms in solution is the same. That is, the equilibrium concentration in a solvent corresponding to dissolution of pentagonal defects should be significantly higher than that corresponding to nanotube hexagons. For instance, the binding energy E_b per one atom in nanotubes is well known to be larger by ≈ 0.4 eV compared to fullerene molecules consisting of pentagons and hexagons. Even taking this average difference, one finds that for $T = 1000-1500$ K the equilibrium solute concentration corresponding to pentagonal defects is about 20–100 times greater than that of NT hexagons. This means that a metal nanoparticle supersaturated with C relative to hexagon formation is undersaturated relative to pentagonal defects and, therefore, should effectively dissolve them if they form on the growth edge.

The involvement of metal nanoparticles provides two additional effects. First, the presence of the metal nanoparticle provides an additional sink for the solidification heat released at the growth edge, which tends to increase NT temperature [46]. This effect inhibits the temperature increase and, hence, the formation of pentagons at the NT growth edge. Second, metal nanoparticles enhance NT nucleation in carbon vapor leading to more intensive carbon condensation. Therefore, together with increasing the edge stability against pentagon formation, the involvement of catalyst nanoparticles as NT nucleation centers additionally provides a fast decrease in C content in the gas phase, causing a decrease in the concentration of C on the SWNT surface, and, thereby, inhibiting next layer nucleation [17].

F. Postnucleation edge stabilization

Let us note that the process of NT growth is closely related to the nucleation stage. The initial NT ring nucleus has been suggested to form from polyyne rings [8], from two parallel carbon sheets evolving into a tube by thermal activation [48], from a semifullerene nucleus [39], from a catalyst nanoparticle [33], by a carbon nanosheet folding into a NT ring nucleus via thermal vibrations [24] or via long-range interaction with a nanoparticle [44]. Whatever the nucleation mechanism, NT growth in the postnucleation stage appears to be due to surface diffusion and the initial ring nucleus may evolve into a continuously growing NT if immediately after the nucleation the open edge is stabilized against pentagon formation. To define the P_c-T area of postnucleation stabilization of the growth edge of the ring nucleus, we show in Fig. 7 the isoline $\tau_p/\tau_h = 10$ calculated for a NT ring nucleus with length $L = 1$ nm. The P_c-T area above this isoline corresponds to the nucleus edge stabilization enabling NT growth, whereas below this line the nucleus edge should be prone to pentagon formation immediately after nucleation, causing termination of NT growth. This figure shows that the growth edge may not be stabilized and the ring nucleus may not evolve into NT growth for $T > 1800$ K even for very high carbon vapor pressures (of the order of 10^4 Pa). This temperature limit is in good agreement with a similar conclusion relevant to the growth of MWNTs based upon other arguments [49].

In addition, the results of a molecular dynamics study show that for a specific temperature and carbon flux onto the growth edge, pentagon formation provoking SWNT closure prevails for small diameters, whereas for large SWNT diam-

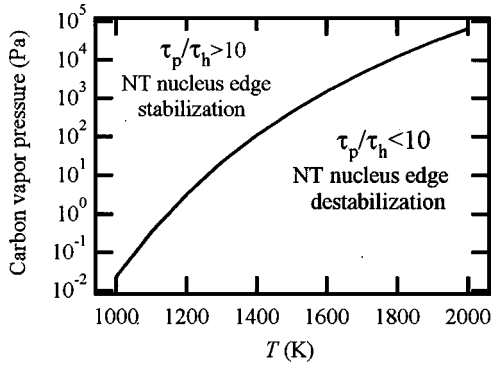

FIG. 7. P_c-T areas corresponding to (i) postnucleation edge stabilization against pentagon formation allowing the initial nuclei to evolve into NTs (above solid line) and (ii) edge destabilization by pentagon formation causing formation of fullerenelike structures.

eters (larger than 3 nm) the edges are not prone to end closure by pentagon formation [37]. This suggests that the activation energy of pentagon defect formation, δE_p, depends also on the radius: the smaller the radius, the smaller the value of δE_p. Hence, the smaller the radius the smaller the characteristic time of pentagon defect formation, τ_p, and consequently smaller would be the hexagon formation time required to inhibit pentagon formation and open-end closure. This explains why the small radii SWNTs do not form without the additional stabilizing effect of metal nanoparticles or hydrogen atoms, which when adsorbed on the edge make it stable with respect to pentagon formation.

It should be also noted here that the possible increase of δE_p with increase in NT radius permits also a simple explanation of experimental observations, showing a shift of nanotube diameter distribution to larger values, taking place with the increase in growth environment temperature [50]. That is, narrow NTs with smaller values of δE_p should be more prone to edge destabilization by pentagon formation and closure with increase in T compared with NTs with larger diameters and larger values of δE_p. Hence, the tendency of narrow diameter NTs to help edge destabilization and closure should obviously decrease their fraction in the final NT output shifting the whole distribution to larger diameters with increase in T.

IV. EDGE STABILIZATION AGAINST DIFFUSION-LIMITED AGGREGATION

A. Perturbation analysis

In addition to the atomic-scale pentagon defects provoking NT closure, there is an additional type of possible morphological destabilization in NT growth found by molecular dynamics studies [42]. In particular, this study shows that an initially even edge of a two-layer NT, held under a flux of C atoms incoming directly from the gas, becomes uneven with time, i.e., covered with large protuberances, transforming into caplike edge structures destabilizing NT growth [Fig. 8(a)]. Thus, if the growth is fed by atoms impinging directly into the edge from the gas, the edge should be prone to this kind of morphological destabilization, making NT assembly

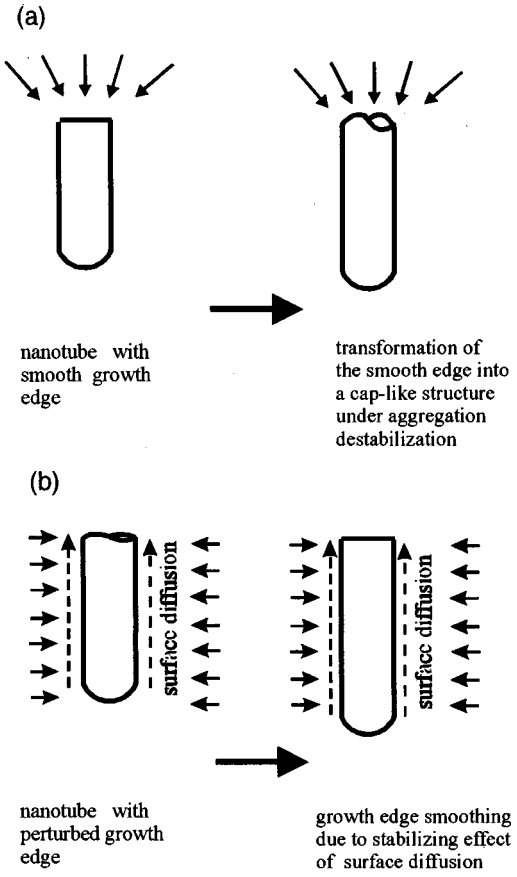

FIG. 8. Schematization of (a) morphological destabilization by direct impingement of atoms into the NT edge and (b) morphological stabilization by the effect of surface diffusion feeding NT growth.

impossible. It should be noted that this kind of instability has long been known to take place in diffusion-limited solid phase formation [51]. For step-flow growth, this kind of instability introduced for the silicon homoepitaxy technique [52] was recently observed [53]. For the case of conditions far from equilibrium, fractal-like growth patterns with branching processes occurring on the scale of the growth unit dimensions are well known [54].

In contrast to the techniques where the diffusion feeding the growth takes place in front of the solidification interface, for the case of NT growth, the surface diffusion feeding the growth from behind the edge has previously been suggested to inhibit this type of edge instability [shown in Fig. 8(b)] [14]. The present analysis treats this problem in more detail, taking into account the possibility of a thermokinetical effect at the NT edge in order to provide a better insight into this kind of destabilization.

The linear perturbation analysis performed below treats the surface concentration field $n(\mathbf{x})$ on the lateral surface described by Eq. (4) together with the balance at the growth edge [55]:

$$-D_s dn/dx = k(n - n_{\mathrm{eq}}^0), \tag{24}$$

where $n_{\mathrm{eq}}^0 \approx \Omega^{-1} \exp(-E_{\mathrm{inc}}/k_B T)$ is an equilibrium concentration, where $E_{\mathrm{inc}} = E_b - E_a$ is the incorporation energy (E_b is the binding energy).

In addition, morphological stability may be caused by the effect of thermal perturbation of the incorporation kinetics at the edge. That is, in the case when the temperature along the NT wall changes near the growth edge, a small edge protuberance, $\cong \delta l$, induces a small temperature perturbation at the tip of this protuberance, $\delta T \cong \delta l \,\mathrm{grad}\, T$, which in turn produces a change in the kinetic constant, $\delta k \cong \delta T\, dk/dT \cong \delta l \,\mathrm{grad}\, T\, dk/dT$. The change in the kinetic constant leads to a corresponding change in the incorporation rate, which leads to kinetic enhancement of the initial protuberance if the temperature increases toward the edge ($\mathrm{grad}\, T > 0$). Therefore, the present analysis includes the temperature field in the wall in the approximation of a thermally thin body,

$$d k_s \nabla^2 T + \Sigma Q_h = 0, \tag{25}$$

where d is the NT wall thickness, k_s is the heat conductance, and ΣQ_h is the heat exchange balance including heat generation and removal occurring on the lateral surface of the NT.

Perturbing the concentration and temperature fields by $\delta H = \varepsilon \exp(\omega t + iay)$ along the edge (y coordinate), one obtains an expression for the perturbation increment ω depending on the perturbation wave number $a = 2\pi/\lambda$ (λ is the perturbation wavelength):

$$\omega = \Omega D_s a \left(G + \frac{n_i - n_{\mathrm{eq}}^0}{k} \frac{dk}{dT} G_T - \frac{dn_{\mathrm{eq}}^0}{dT} G_T - \frac{n_{\mathrm{eq}}^0 \Omega \gamma a^2}{k_B T} \right), \tag{26}$$

where $G = \mathbf{e}\nabla n$ is the value of the concentration gradient at the growth edge and $\mathbf{e}$ is a normal unit vector pointing outwards from the edge in the positive x direction, $G_T = \mathbf{e}\nabla T$ is the temperature gradient at the edge, $k^{-1} dk/dT = \delta E_{\mathrm{inc}}/(k_B T^2)$ and $dn_{\mathrm{eq}}^0/dT = n_{\mathrm{eq}}^0 E_{\mathrm{inc}}/(k_B T^2)$.

The activation energy of incorporation is the energy barrier the adatom has to overcome to make a transition from the surface near the edge onto the edge. Reference [19] does not show that there is any additional energy barrier except that of surface diffusion, that is, $\delta E_{\mathrm{inc}} \approx \delta E_D \approx 0.13$ eV. The value of surface energy at the edge is $\gamma \cong 10$ eV/nm. The value of G_T is defined by the energy balance at the edge:

$$k_s G_T \approx V E_{\mathrm{inc}}/(\Omega d), \tag{27}$$

where k_s is the heat conductance of the NT wall and d is the NT wall thickness. This equation contains only a part of the binding energy, $E_{\mathrm{inc}} = E_b - E_a$, because the adsorption energy $E_a \approx 1.8$ eV [19] produces the corresponding thermal effect on the lateral surface of a carbon NT.

B. Morphological stabilization

In Fig. 9 we show the values of all the terms included in dispersion equation (26) calculated for SWNT growth for

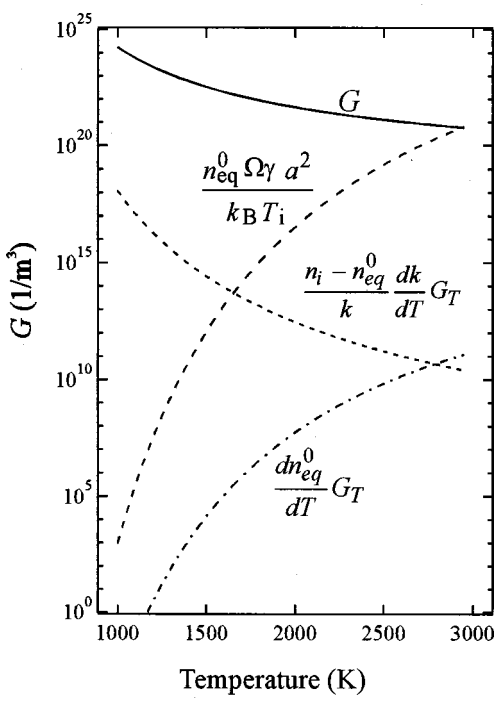

FIG. 9. Estimates of different terms in the perturbation increment Eq. (26) as a function of growth temperature.

$P_c = 4$ Pa ($T_{\mathrm{ev}} = 3000$ K), $T = 1000$–2900 K, and a perturbation wavelength $\lambda = 1$ nm. The concentration gradient is estimated as $G = \mathbf{e}\nabla n = V/\Omega D_s$ and $n_i - n_{\mathrm{eq}}^0 = V/k\Omega$, where V is estimated by the steady-state growth approximation (the NT length becomes larger than the diffusion length):

$$V \approx \frac{\Omega k (Q_c \tau_a - n_{\mathrm{eq}}^0)}{1 + k(\tau_a/D_s)^{1/2}}. \tag{28}$$

This figure shows that the term corresponding to the gradient of surface concentration prevails by several orders of magnitude over all other terms in the dispersion equation (26). Only when T is close to that of evaporation, 3000 K, the surface energy term $n_{\mathrm{eq}}^0 \Omega \gamma a^2/(k_B T)$ attains the order of magnitude of G. The value of the heat conductance is assumed to be that of graphite perpendicular to the c axis, that is, $k_s \approx 250$ W/mK (for $T = 2000$ K) [56]. Taking into account that for a NT wall k_s may be significantly higher [57] than that of graphite, the values of the two terms associated with $G_T \propto 1/k_s$ appear even smaller.

Equation (26), which includes thermal effects, provides an interpretation of a molecular dynamics simulation of NT growth revealing the formation of edge undulations [42]. In this study the edge was subjected to a direct flux of atoms implying that the value of $G = 0$. However, the NT fragment in the simulations was kept under an extremely high temperature gradient $G_T \approx 10^{12}$ K/m (from 3000 K at the edge to 1700 K at the bottom part of the NT fragment of 12 atomic layers). This suggests that the destabilization found in this study would be probably caused by thermokinetical perturbation at the edge, i.e., by a term $\propto G_T dk/dT$, where k is also

defined by the Arrhenius type expression similar to that of Eq. (12). It is difficult to determine from Ref. [42] the characteristic kinetic path of atom incorporation, but at least the stage of the bond switching into hexagon formation is similar to Eq. (12), $\propto \nu \exp(-\Delta/k_B T)$, where $\Delta \approx 1.55$ eV [38]. This kind of destabilization cannot be smoothed out by diffusion over the edge. In effect, the activation energy of C atom diffusion over the edge, 2.4 eV [19], shows that the C atoms impinged onto the edge at a rate of one atom per 290 ps, whereas the diffusion time at the edge for 3000 K is about $v^{-1} \exp(2.4\ \text{eV}/k_B T) \cong 350-1000$ ps. For lower T the situation is similar: for $T=1500$ K and growth rate $V=0.1$ mm/s [19] the period of time during which one atom incorporates into one site is $\cong a_0/V \cong 1\ \mu$s, whereas the time required for atom relocation to a neighboring site on the edge is $\cong 10\ \mu$s.

In reality (especially for low temperatures) a particular mode of thermokinetical destabilization should not be expected in NT growth. Moreover, our recent thermal physics estimates show that the temperature of carbon nanotubes remains practically uniform as long as the NT length is smaller than $\approx 1-10\ \mu$m [46]. However, the edge may be destabilized by random growth fluctuations, atom aggregation, or by condensation of large carbon fragments. In this case Eq. (26) reduces to

$$\omega \simeq 2\pi\Omega\lambda^{-1} D_s G, \tag{29}$$

which shows that in the case of NT growth fed by diffusion "from behind" the edge, $G=\mathbf{e}\nabla n<0$, and, therefore, $\omega<0$ for all λ, implying that possible perturbations of the growth edges caused by aggregation or cluster deposits onto the edge should decay, and with time this perturbation is smoothed out [as schematized in Fig. 8(b)]. Figure 10(a) shows the value of ω versus λ on the NT edge for $P_c=4$ Pa and $T=1200$ and 1500 K. In this case, $G=\mathbf{e}\nabla n<0$ and, therefore, the open end is stable relative to perturbations of all wavelengths. The fastest decay corresponds to the smallest possible perturbation of the scale of one growth unit $\lambda=a_0$, i.e., to one C atom. That is, the growth edge of a NT end has a tendency to equalize itself even relative to atomic-scale unevenness. Hence, NT growth fed by surface diffusion provides an intrinsic morphological stabilization of the edge of the open end, compared with crystal growth patterns, where the feeding species diffuse in front of the growth interface implying $G=\mathbf{e}\nabla n>0$ and $\omega>0$. This allows us to conclude that the open edge should normally remain even during the growth of NTs and that randomly occurring perturbations should be smoothed with time. In contrast, Fig. 10(b) represents an alternative case, i.e., when the growth is fed in front of the interface, $G=\mathbf{e}\nabla n>0$, and, therefore, the growth edge becomes unstable and the maximal increment corresponds to an atomic-scale perturbation. Thus, without the effect of surface diffusion, the stable growth of NTs with an open end would not be feasible.

C. Morphological destabilization in MWNT growth

Nevertheless, the growth edges may be prone to this kind of perturbation during the formation of MWNTs by a step-flow growth mode. In effect, when the layer propagates along the underlying layer the stability of the growth edge is determined by the interference of diffusion fluxes feeding the layer from both sides of the edge. The increment of the perturbation of layer number i, ω_i, is given in this case by

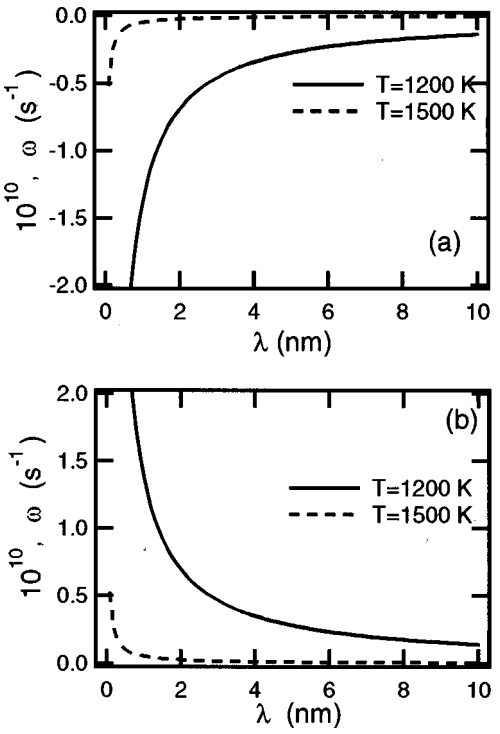

FIG. 10. Perturbation increment of the NT layer edge fed by surface diffusion (a) from behind the edge and (b) in front of the edge as a function of the perturbation wavelength.

$$\omega_i \simeq 2\pi\Omega\lambda^{-1} D_s (G_i + G_{i-1}), \tag{30}$$

where $G_i=\mathbf{e}\cdot\nabla n_i<0$ and is the concentration gradient at the edge on its own surface, whereas $G_{i-1}=\mathbf{e}\nabla n_{i-1}>0$ is the concentration gradient at the edge on the underlying layer.

This expression shows that in the step flow of MWNTs, the layers undergo a transition from morphological instability to stability. That is, immediately after the nucleation of every new layer its edge is unstable against perturbation ($\omega_1>0$), whereas with time it becomes stable ($\omega_1<0$). This effect happens because the new layer is initially fed by the surface diffusion in front of its edge from the underlying layer when it nucleates on the surface of the previous layer. This takes place in the growth of a MWNT starting from a semifullerene nucleus (or small particle) immediately after the nucleation when the second layer surface is small [Fig. 11(a)]. In this case the growth edge moves in the direction of the increase in the feeding surface concentration and, therefore, $\omega_2 \propto G_1=\mathbf{e}\nabla n_1>0$, and it is unstable with respect to perturbations. But when the layer becomes large enough, and when its edge gets closer to the edge of the underlying layer [Fig. 11(b)] it is mainly fed by the surface diffusion from its own surface—from "behind the edge" and $\omega_2 \propto G_2=\mathbf{e}\nabla n_2<0$. This means that the edge perturbation of a new layer

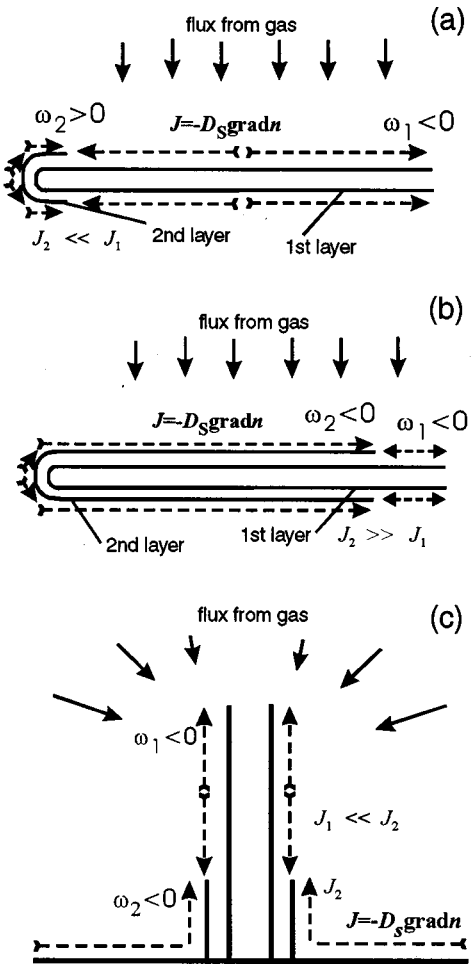

FIG. 11. Schematization of layer-by-layer growth of MWNTs: the edge of the second layer (a) after the nucleation is fed by large surface diffusion flux causing morphological destabilization of the edge (b), whereas when the edge of the second layer reaches that of the previous one it is mainly fed by surface diffusion from behind providing morphological stabilization of the edge; (c) in NT growth from a substrate the edge of the external layer is not prone to morphological destabilization even after nucleation because it is mainly fed by surface diffusion from an underlying substrate.

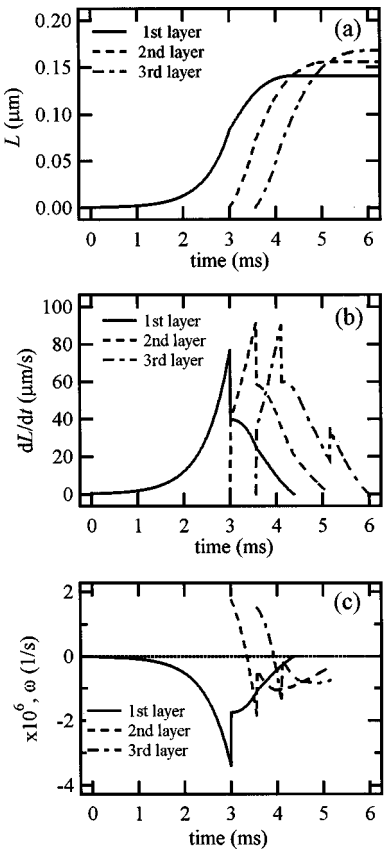

FIG. 12. Layer-by-layer MWNT growth by the surface diffusion mechanism starting from a semifullerene particle as a function of time: (a) layer lengths, (b) layer growth rates, and (c) perturbation increment for perturbation wavelength $\lambda=a_0$. The simulation is done for the growth temperature $T=1500$ K and $P_c=4$ Pa.

which may develop immediately after its nucleation should be smoothed out when the length of this layer becomes larger. Finally, it is worth noting that in step-flow growth of a MWNT from the surface of a substrate shown in Fig. 11(c), the edges of the next layers are not prone to morphological destabilization even after the nucleation, because the external layer is fed from behind by the diffusion flux from the substrate, which is significantly larger that the flux from the previous layer, providing $\omega<0$ for all layers.

This analysis is supported by the simulation of MWNT growth in step-flow mode, which shows that during the growth the layer edges are initially prone to this instability. The results of this simulation are shown in Figs. 12(a)–12(c), including (a) layer lengths, (b) layer growth rates, and (c) perturbation increment estimated for $\lambda=a_0$. The growth of the first layer is started from a semifullerene cluster, whereas all subsequent layers are triggered when the surface concentration attains a critical level of nucleation. The numerical model and computational details are given in Ref. [17]. Figure 12(c) shows that the first layer is stable from the beginning until the growth termination, which occurs when it is overtaken by the second layer. In contrast to this, all subsequent layers are prone to instability directly after the nucleation ($\omega_2>0$ and $\omega_3>0$). However, with increase in the layer lengths the growth edges become and later remain morphologically stable ($\omega_2<0$ and $\omega_3<0$) until the termination of their growth.

V. SUMMARY AND CONCLUSIONS

The above analysis shows that, in addition to the many previously discussed effects, the mechanism of surface diffusion stabilizes the edge of an open-ended NT against growth perturbations of two kinds: (i) pentagon defects and (ii) morphological destabilization caused by atom aggregation.

The stability of the NT end against closure is determined by the competition of two processes (i) thermally activated pentagon defect formation, which initiates the closure, and (ii) regular hexagon network formation, which depends on the repetition rate at which the new carbon atoms are fed to

the growth edge by the mechanism of surface diffusion. The nanotube has a tendency to close itself up when the first process has a shorter characteristic time, i.e., when the pentagons at the edge are formed even before new atoms come to the edge to form regular hexagons. Therefore, the growing open-ended nanotubes close themselves up whenever the change in the growth conditions (temperature, carbon vapor pressure, and surface area of nanotube wall from which the open end is fed) decreases the surface diffusion flux at the edge to the level at which the characteristic time between new atom arrivals on the edge and the formation of regular hexagons becomes larger than the characteristic time of pentagon defect formation. All these processes increase the characteristic time at which the atoms are fed to the edge. If this time becomes large enough compared with the time of pentagon formation, this would initiate NT closure explaining why the majority of NTs grow open ended and then close up at the end of the process when C pressure falls down.

By virtue of this effect, the edge of the open-ended NT, if it is fed by a sufficiently large surface diffusion flux, may remain stable even without additional effects such as catalyst or lip-lip interaction with another layer. However, this situation may change during the growth for several reasons: a fall in carbon vapor pressure, transport of the NT into an area of low pressure or high temperature, and new layer nucleation and growth, which with time decreases the surface diffusion flux feeding the underlying layer. We note that the mechanism proposed in Sec. III B for open-end closure in MWNT layer-by-layer growth occurring when the upper layer approaches the underlying layer is in good agreement with a microscopic image of a three layer WS_2 nanotube [58], which exhibits an open-end bent inwards in the presence of the edge of the third external layer.

The growth of SWNT as well as transition from SWNT to MWNT is shown to be at the nexus of two conflicting criteria. That is, edge stabilization against pentagon formation requires an increase in the carbon vapor pressure P_c and decrease in growth temperature T, whereas in order to inhibit secondary nucleation on the surface of the first layer, it is necessary to decrease P_c and to increase T. A parametric study of both criteria distinguishes particular P_c-T areas where growth of SWNTs may be feasible. In particular, SWNT formation is feasible only when its length is much smaller than that of the diffusion length, and the surface concentration of C adatoms remains too low to trigger the nucleation of a new layer. However, with increase in SWNT length (i) it is prone to the formation of further layers leading to MWNT formation (under high P_c and low T), or (ii) it is prone to edge destabilization and closure (under low P_c and high T). However, the additional stabilizing effects at the edge, effectively inhibiting pentagon defect formation, may allow long SWNTs (longer than the surface diffusion length) to form even under low P_c. In particular, attached metal nanoparticles produce three additional effects. First, the presence of metal particles at the NT growth edge inhibits the formation of pentagons under pressure-temperature conditions at which, without them, the NT open edge would be prone to destabilization. Second, the presence of the catalyst nanoparticle provides an additional sink for the solidification heat released at the growth edge. This effect inhibits the temperature increase and, hence, the formation of pentagons at the NT growth edge. Third, the presence of metal nanoparticles enhances NT nucleation in the vapor, leading to more intensive C vapor condensation. Together with increasing the edge stability against pentagon formation, the involvement of metal nanoparticles as NT nucleation centers leads to a fast decrease in C content in the gas phase, causing a decrease in P_c on the SWNT surface, and thus inhibition of next layer nucleation.

The parametric study of edge stability against pentagon formation performed for a small NT ring nucleus (1 nm long) suggests that there is an upper temperature limit for edge stabilization of such nuclei against pentagon formation. For instance, for $P_c \approx 10^4$ Pa this temperature is about $\approx$1800 K. Above this temperature limit the nucleus should not evolve into nanotube growth, transforming rather into fullerenelike and other particles. This shows that the molecular dynamics studies of nanotube growth kinetics based upon *ab initio* and semiempirical potentials, performed at 3000 K, may not adequately represent the kinetic paths in NT assembly, which obviously take place at significantly lower temperatures. A recent molecular dynamics study based on analytical forms of interatomic potentials for carbon and metal catalysts [59] shows that under high temperature ($>$2000 K) the formation of cagelike nanoparticles containing many defects takes place, instead of nanotube formation.

In connection with the initial stage of NT formation we note the results of a recent study of aligned NT growth on SiC by ''the surface decomposition method,'' showing that NT length increases parabolically and exponentially as a function of heating time and temperature, respectively [60]. This result is in good agreement with the surface diffusion model. That is, the exponential increase of the growth rate with increase in T is defined by the exponential dependence of the carbon vapor pressure on T, whereas the parabolic increase in NT length with time is an intrinsic feature of the initial stage of NT growth mediated by surface diffusion, as the growth rate is proportional to NT length as defined by Eqs. (8) and (9).

We would also like to add that the proposed mechanism of kinetic competition between pentagon defects and regular hexagons resolves not only the particular problem of edge stability in NT growth, but also the problem of kinetic selection between NT and fullerenelike nanoparticle formation [46]. In our opinion, it may resolve a more general problem of kinetic selection between the formation of the fullerene and graphitic phases—a problem which still remains unresolved in terms of thermodynamics and structural energetics. We suggest here that the selection between the graphite and fullerene phase formation is also defined by a competition of pentagon and hexagon formation, which takes place at the initial stage of hexagon cluster extension by C condensation from vapor, i.e., when the first pentagonal defect is formed via a thermally activated process at the edge of two or three neighboring hexagons, initiating the bending of the plane sheet into a nanospherical cluster.

The perturbation analysis of the growth edge stability

based on an NT growth model mediated by surface diffusion along the external surface allows a transparent explanation of the stabilization of the NT edge against perturbations caused during growth by atom aggregation, cluster deposition on the edge, or by thermal perturbation of the incorporation kinetics. This analysis shows that without the mechanism of surface diffusion, which effectively smoothes out this kind of perturbation, this edge stabilization and the stable open-ended growth of long NTs would not be feasible.

ACKNOWLEDGMENTS

The authors would like to thank Dr. J. Hester for reading this manuscript and for providing them with numerous valuable suggestions. The continued financial support for this work to O.A.L. within the framework of The Center of Excellence Project of The National Institute for Materials Science (formerly National Institute for Research in Inorganic Materials) is gratefully acknowledged.

[1] S. Iijima, Nature (London) **354**, 56 (1991).
[2] S. Iijima, P. M. Ajayan, and T. Ichihashi, Phys. Rev. Lett. **69**, 3100 (1992).
[3] T. W. Ebbesen and P. M. Ajayan, Nature (London) **358**, 220 (1992).
[4] P. M. Ajayan, Prog. Cryst. Growth Charact. Mater. **38**, 37 (1997).
[5] S. Iijima, Mater. Sci. Eng., B **19**, 172 (1993).
[6] C.-H. Kiang, W. A. Goddard III, R. Beyers, J. R. Salem, and D. S. Bethune, J. Phys. Chem. **98**, 6612 (1994).
[7] X. F. Zhang, X. B. Zhang, G. Van Tendeloo, S. Amelinckx, M. Op de Beeck, and J. Van Landuyt, J. Cryst. Growth **130**, 368 (1993).
[8] C. H. Kiang and W. A. Goddard III, Phys. Rev. Lett. **76**, 2515 (1996).
[9] T. M. Endo and H. W. Kroto, J. Phys. Chem. **96**, 6941 (1992).
[10] R. Saito, G. Dresselhaus, and M. S. Dresselhaus, Chem. Phys. Lett. **195**, 537 (1992).
[11] C. J. Brabec, A. Maiti, C. Roland, and J. Bernholc, Chem. Phys. Lett. **236**, 150 (1995).
[12] S. Amelinckx, X. B. Zhang, D. Bernaerts, X. F. Zhang, V. Ivanov, and J. B. Nagy, Science **265**, 63 (1994).
[13] E. G. Gamally and T. W. Ebbesen, Phys. Rev. B **52**, 2083 (1995).
[14] O. A. Louchev, Appl. Phys. Lett. **71**, 3522 (1997).
[15] O. A. Louchev and Y. Sato, Appl. Phys. Lett. **74**, 194 (1999).
[16] O. A. Louchev, Y. Sato, H. Kanda, and Y. Bando, Appl. Phys. Lett. **77**, 1446 (2000).
[17] O. A. Louchev, Y. Sato, and H. Kanda, J. Appl. Phys. **89**, 3438 (2001).
[18] O. A. Louchev, J. Cryst. Growth **65**, 237 (2002).
[19] Y. H. Lee, S. G. Kim, and D. Tomanek, Phys. Rev. Lett. **78**, 2393 (1997).
[20] L. T. Chadderton and Y. Chen, Phys. Lett. A **263**, 401 (1999).
[21] O. A. Louchev, Y. Sato, and H. Kanda, Appl. Phys. Lett. **80**, 2752 (2002).
[22] A. Gorbunov, O. Jost, W. Pompe, and A. Graff, Carbon **40**, 113 (2002); Appl. Surf. Sci. (to be published).
[23] R. T. K. Baker and P. S. Harris, in *Chemistry and Physics of Carbon*, edited by P. L. Walker, Jr. and P. A. Thrower (Marcel Dekker, New York, 1978), pp. 83–161; A. Oberline, M. Endo, and T. Koyama, J. Cryst. Growth **32**, 335 (1976); G. G. Tibbetts, *ibid.* **66**, 632 (1984).
[24] E. Gamaly, A. V. Rode, W. K. Maser, E. Muñoz, A. M. Benito, M. T. Martínez, and G. G. de la Fuente, Appl. Phys. A: Mater. Sci. Process. **A70**, 161 (2000).
[25] E. Gamaly, A. V. Rode, W. K. Maser, E. Muñoz, A. M. Benito, M. T. Martínez, and G. G. de la Fuente, Appl. Phys. A: Mater. Sci. Process. **A69**, S121 (1999).
[26] A. A. Puretzky, D. B. Geohagen, X. Fan, and S. J. Pennycook, Appl. Phys. Lett. **76**, 182 (2000).
[27] A. A. Puretzky, D. B. Geohagen, X. Fan, and S. J. Pennycook, Appl. Phys. A: Mater. Sci. Process. **A70**, 153 (2000).
[28] A. V. Latuyshev, A. L. Aseev, A. B. Krasilnikov, and S. I. Stenin, Surf. Sci. **213**, 157 (1989).
[29] R. E. Smalley, Mater. Sci. Eng., B **19**, 1 (1993).
[30] A. Maiti, C. J. Brabec, C. M. Roland, and J. Bernholc, Phys. Rev. Lett. **73**, 2468 (1994).
[31] M. Ge and K. Sattler, Appl. Phys. Lett. **65**, 2284 (1994); Science **260**, 515 (1993); L. A. Chernozatonskii, Z. Ya. Kosakovskaja, A. N. Kiselev, and N. A. Kiselev, Chem. Phys. Lett. **228**, 94 (1994).
[32] M. Endo, K. Takeuchi, S. Igarashi, K. Kobori, M. Shiraishi, and H. W. Kroto, J. Phys. Chem. Solids **54**, 1841 (1993); N. Hatta and K. Murata, Chem. Phys. Lett. **217**, 398 (1994); J. B. Howard, K. D. Chowdhury, and J. B. VanderSande, Nature (London) **370**, 603 (1994).
[33] D. S. Bethune, C. H. Kiang, M. S. de Vries, G. Gorman, R. Savoy, J. Vazquez, and R. Beyers, Nature (London) **363**, 605 (1993).
[34] A. Thess, R. Lee, P. Nikolaev, H. Dai, P. Petit, J. Robert, C. Xu, Y. H. Lee, S. G. Kim, A. G. Rinzler, D. T. Colbert, G. E. Scuseria, D. Tomanek, J. E. Fischer, and R. E. Smalley, Science **273**, 483 (1996).
[35] J. Ch. Charlier, X. Blase, A. De Vita, and R. Car, Appl. Phys. A: Mater. Sci. Process. **A68**, 276 (1999).
[36] X. Blase, J.-C. Charlier, A. De Vita, R. Car, Ph. Redlich, M. Terrones, W. K. Hsu, H. Terrones, D. L. Caroll, and P. M. Ajayan, Phys. Rev. Lett. **83**, 5078 (1999).
[37] A. Maiti, C. J. Brabec, C. M. Roland, and J. Bernholc, Phys. Rev. Lett. **73**, 2468 (1994).
[38] A. Maiti, C. J. Brabec, C. Roland, and J. Bernholc, Phys. Rev. B **52**, 14 850 (1995).
[39] T. Guo, P. Nikolaev, A. G. Rinzler, D. Tomanek, D. T. Colbert, and R. E. Smalley, J. Phys. Chem. **99**, 10 694 (1995).
[40] Y.-K. Kwon, Y. H. Lee, S. G. Kim, P. Jund, D. Tomanek, and R. E. Smalley, Phys. Rev. Lett. **79**, 2065 (1997).
[41] J. C. Charlier, A. De Vita, X. Blase, and R. Car, Science **275**, 646 (1997).
[42] M. B. Nardelli, C. Brabec, A. Maiti, C. Roland, and J. Bernholc, Phys. Rev. Lett. **80**, 313 (1998).
[43] K. A. Williams, M. Tachibana, J. L. Allen, L. Grigorian, S.-C.

Cheng, S. L. Fang, G. U. Sumanasekera, A. L. Loper, J. H. Williams, and P. C. Eklund, Chem. Phys. Lett. **310**, 31 (1999).
[44] J. R. Hester and O. A. Louchev, Appl. Phys. Lett. **80**, 2580 (2002).
[45] F. Okuyama and I. Ogasawara, Appl. Phys. Lett. **71**, 623 (1997).
[46] O. A. Louchev, Y. Sato, and H. Kanda, J. Appl. Phys. **91**, 10074 (2002).
[47] H. Cui, O. Zhou, and B. R. Stoner, J. Appl. Phys. **88**, 6072 (2000).
[48] P. Zhang and V. H. Crespi, Phys. Rev. Lett. **83**, 1791 (1999).
[49] V. Crespi, Phys. Rev. Lett. **82**, 2908 (1999).
[50] S. Bandow, S. Asaka, Y. Saito, A. M. Rao, L. Grigorian, E. Richter, and P. C. Eklund, Phys. Rev. Lett. **80**, 3779 (1998).
[51] W. W. Mullins and R. F. Sekerka, J. Appl. Phys. **35**, 444 (1964).
[52] G. S. Bales and A. Zangwill, Phys. Rev. B **41**, 5500 (1990).
[53] P. Finnie and Y. Homma, Phys. Rev. Lett. **85**, 3237 (2000).
[54] T. A. Witten and L. M. Sander, Phys. Rev. Lett. **47**, 1400 (1981).
[55] This expression is obtained for the general case of near equilibrium growth, including also the perturbation of the equilibrium concentration in front of the edge due to edge curvature, given by the Gibbs-Thompson relationship $n_{eq}=n_{eq}^{0}\exp(-\Omega\gamma\kappa/k_BT)$, where $\kappa\cong d^2\delta H/dy^2=-\varepsilon a^2\exp(\omega t)\sin(ay)$.
[56] Y. S. Touloukian, *Thermophysical Properties of Matter* (Plenum, New York, 1970), Vol. 2, p. 41.
[57] S. Berber, Y.-K. Kwon, and D. Tomanek, Phys. Rev. Lett. **84**, 4613 (2000).
[58] M. Kociak, O. Stéphan, L. Henrard, V. Charbois, A. Rothshild, R. Tenne, and C. Colliex, Phys. Rev. Lett. **87**, 075501 (2001).
[59] Y. Shibuta and S. Maruyama, *Book of Abstracts of Tsukuba Symposium on Carbon Nanotubes* (Tsukuba, Japan, 2001); Physica B (to be published).
[60] M. Kusunoki, T. Suzuki, C. Honjo, T. Hirayama, and N. Shibata, *Book of Abstracts of Tsukuba Symposium on Carbon Nanotubes* (Ref. [59]); Physica B (to be published).